

# Dynamic Light Scattering and Dynamic Viscoelasticity of Poly(vinyl alcohol) in Aqueous Borax Solutions. 1. Concentration Effect

Akihiro Koike,\*<sup>†</sup> Norio Nemoto,<sup>†</sup> Tadashi Inoue, and Kunihiro Osaki

*Institute for Chemical Research, Kyoto University, Uji, Kyoto 611, Japan*

*Received August 30, 1994; Revised Manuscript Received January 10, 1995\**

**ABSTRACT:** This paper presents dynamic light scattering (DLS) and dynamic viscoelasticity (DVE) studies on transparent aqueous solutions of poly(vinyl alcohol) (PVA) and sodium borate (SB) with a ratio of 2 to 1 by weight fraction. The PVA concentrations,  $C$ , of the samples tested are 1.5, 1.8, and 2.0 wt %. The time correlation function,  $A_q(t)$ , of light intensity scattered from the samples always exhibits a bimodal distribution of the decay rate,  $\Gamma$ . The fast and the slow modes are the diffusive modes for the sample with  $C = 1.5$  wt %, slightly higher than the overlapping concentration at 25.0 °C. At higher concentrations of  $C = 1.8$  and 2.0 wt %, where the samples behaved like weak gels, the fast and the slow modes are found to be a cooperative diffusion and a relaxation mode, respectively. The characteristic relaxation time,  $\tau_s$ , estimated for the slow mode is in good agreement with the mechanical relaxation time,  $\tau_M$ , obtained by fitting DVE data to the Maxwell model with a single relaxation time. The agreement is also gratifying at  $T = 35.0$  and 40.0 °C for the sample with  $C = 2.0$  wt %. The results confirm the presence of dynamical coupling between concentration fluctuation and elastic stress in this viscoelastic network system.

## Introduction

Semidilute aqueous solutions of PVA are viscoelastic liquids, and concentrated solutions behave as a physical gel at low temperatures. Remarkable enhancement in viscosity by addition of a small amount of sodium borate (SB) occurs in aqueous solutions of poly(vinyl alcohol) (PVA).<sup>1</sup> This is due to formation of a complex between ols and a borate anion, which plays the role of a transient cross-linker among the PVA chains. Similar behavior by addition of SB has been reported for several other polyhydroxy polymers such as poly(glyceryl methacrylate)<sup>2</sup> and polysaccharides.<sup>1,3,4</sup> Most of the experimental studies concerning these systems have been aimed at either elucidating the ol–borax complex formation mechanism by <sup>11</sup>B-NMR<sup>5–7</sup> or at drawing the phase diagram of the sol–gel transition.<sup>8–10</sup> In these studies, the effects of polymer and borate concentrations, ionic strength, pH, and temperature were discussed. Viscosity measurements were also made for investigation of a relationship between the shear-thickening effect and the complex formation.<sup>8,9,11,12</sup> For semidilute PVA/SB solutions, the shear-thickening phenomenon was observed in steady flow and also in shear creep measurements by our group<sup>13</sup> and by Savins.<sup>14</sup> These results were discussed in relation to the relaxation time distribution observed by the dynamic viscoelastic measurements.

A light scattering study on the transparent PVA/SB system has not yet been conducted. Dynamic light scattering measurements, which measure decay rates of concentration fluctuation in solution, give us information about various molecular motions of polymer chains such as the translational diffusion, the rotational diffusion, and the intramolecular relaxation at the infinite dilution limit. In the semidilute and the concentrated regions where polymer chains extensively overlap one

another, DLS proves cooperative diffusion motion of the network, which may be called the fast mode. The presence of the very slow decay of concentration fluctuation, here called the slow mode, was found for semidilute and concentrated solutions of macromolecules in poor or  $\Theta$  solvent.<sup>21–26</sup> The slow relaxation mode has also been detected<sup>16</sup> on the thread-like micellar system formed by the cationic surfactant cetyltrimethylammonium bromide in aqueous sodium salicylate solutions. Since the dynamical behavior of the micellar network was quite different from that of the entanglement network of high molecular weight polymer chains,<sup>17–20</sup> the above finding suggests that the slow mode may be observed for another viscoelastic network such as a physically cross-linked polymer network.

At present, there are two theoretical ideas for interpretation of the slow relaxation mode. Wang argues that the difference in partial specific volumes of the polymer and the solvent gives rise to dynamical coupling between concentration fluctuation and density fluctuation, and then the viscoelastic mode appears in the DLS power spectrum.<sup>29,30</sup> On the other hand, a couple of theories<sup>27,28,31</sup> predict that mass flow or concentration fluctuation in the gel-like solutions induces deformation of the viscoelastic network and consequently concentration fluctuation may slowly decay out as the elastic stress generated by the network deformation relaxes. These two ideas are essentially incompatible with each other and the physics underlying the slow mode is of issue in the DLS study of viscoelastic polymeric liquids.

This paper reports results of DLS and DVE measurements on semidilute solutions of PVA/SB with PVA concentrations  $C = 1.5$  and 1.8 wt % at 25.0 °C and a 2.0 wt % PVA solution at 25.0, 35.0, and 40.0 °C. One big advantage of this solution compared with polymer entanglement networks in measuring dynamic viscoelasticity is that the former shows nearly a single relaxation behavior, whereas the latter shows a viscoelastic behavior characteristic of a very broad distribution of relaxation times. In the case of the single relaxation behavior, the theory is considerably simplified and a more unambiguous conclusion can be drawn

\* To whom correspondence should be addressed.

<sup>†</sup> Present address: Department of Applied Physics, Faculty of Engineering, Kyushu University, 6-10-1 Hakozaki, Higashiku, Fukuoka 812, Japan.

© Abstract published in *Advance ACS Abstracts*, March 1, 1995.

from detailed comparison between theoretical predictions and experimental data. The results prove the presence of the dynamical coupling in this temporarily cross-linked network.

## Experimental Section

**Materials.** The poly(vinyl alcohol) (PVA) sample used in this study is a gift from Kuraray Co., Ltd. The degree of polymerization is 1750, and the degree of saponification is 96.0 mol %. The polymer was dissolved in dust-free purified water (resistance >16 MΩ), and the concentration of the stock solution was 4.0 wt %. The 2.0 wt % stock solution of sodium borate (SB), Na<sub>2</sub>B<sub>4</sub>O<sub>7</sub>·10H<sub>2</sub>O, was prepared using reagent grade SB (Nacalai Tesque, Inc., Japan). Before mixing, the stock PVA and SB solutions and water were made optically clean by filtration with a Millipore filter (nominal pore size, 0.22 μm) and poured into the DLS cell. To make samples homogeneous and transparent, the mixture were rotated at 0.2 rpm for about 2 h at 80 °C. The final PVA concentrations, *C*, of the samples were 1.5, 1.8, and 2.0 wt %. The sodium borate concentration is half that of PVA by weight.

Maerker and Sinton<sup>5</sup> reported that the shear viscosity of the PVA/SB system was gradually reduced with the elapse of time during a few weeks. They attributed this reduction to hydrolysis of the residual acetic groups of PVA. Because we are interested in the comparison of DLS and DVE results obtained for the sample with identical chemical structure, we performed all measurements within 1 or 2 days after sample preparation. Repeated DLS and DVE measurements after the first run gave the same results.

**Methods.** Dynamic light scattering (DLS) measurements were made with an instrument reported elsewhere.<sup>32</sup> A vertically polarized single-frequency 488 nm line of an argon ion laser (Spectra Physics, Beamlock 2060) was used as a light source with an output power of 400 mW. The normalized time correlation function,  $A_q(t)$ , of the vertical component of the light intensity scattered from the solutions was measured using a digital correlator (Otsuka Electronics) at 12 fixed scattering angles ranging from 10.4 to 150°. The experiments were conducted at 25.0 °C for *C* = 1.5 and 1.8 wt % and at 25.0, 35.0, and 40.0 °C for *C* = 2.0 wt %.

Dynamic viscoelastic (DVE) measurements were made immediately after DLS measurement with a stress-controlled rheometer, CLS-100 (Carri-MED, ITS Japan), using a cone-and-plate geometry with a cone diameter of 4 cm and a cone angle of 2°. The complex modulus was found to be independent of the strain applied when the strain was less than 0.7. This is in accord with results of Schultz and Myers.<sup>33</sup> The storage and the loss shear moduli,  $G'(\omega)$  and  $G''(\omega)$ , of the samples were measured at a strain of 0.3 over an angular frequency,  $\omega$ , range from 0.15 to 100 rad/s at 25.0 °C for *C* = 1.5 and 1.8 wt % and at 25.0, 35.0, and 40.0 °C for *C* = 2.0 wt %, as measured with DLS. A humidity chamber was used to prevent solvent evaporation.

## Results and Discussion

**1. Time Profiles of the Time Correlation Function,  $A_q(t)$ .** Since our correlator has a simple linear channel spacing (maximum channel number of 1024), a single run with one sampling time,  $\Delta\tau$ , could not provide  $A_q(t)$  data sufficient for precise data analysis over a very broad  $\Gamma$  range. Therefore we measured  $A_q(t)$  repeatedly by varying  $\Delta\tau$  by more than 2 orders of magnitude and obtained a composite curve from superposition of a couple of  $A_q(t)$  data. Figure 1 shows, as a typical example, composite curves thus obtained for the sample with *C* = 2.0 wt % at scattering angles,  $\theta$ , of 15, 30, and 150°. As is seen from the figure, the time profile of  $A_q(t)$  was represented by a bimodal distribution of the decay rate. Since the fast mode was well separated from the slow mode in the time scale, we applied the cumulant analysis to the data in the short-time domain

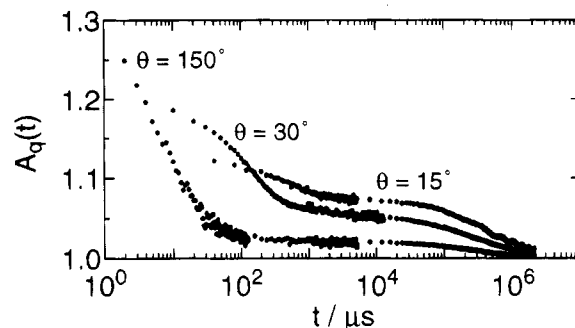


**Figure 1.** Time profiles of the normalized time correlation function,  $A_q(t)$ , for the PVA/SB system with *C* = 2.0 wt % at 25.0 °C. Scattering angles  $\theta$  are 15, 30, and 150°. The curves are composite ones obtained by superposition of two or three raw  $A_q(t)$  data with different sampling times.

to obtain the first cumulant,  $\Gamma_f$ , characteristic of the fast mode.

$$A_q(t) = \beta + A_f |g_q^{(1)}(t)|^2 \quad (1)$$

$$\ln |g_q^{(1)}(t)| = \sum K_m(\Gamma_q)(-\tau)^m/m! \quad (2)$$

$$\Gamma_f = K_1(\Gamma_q) \quad (3)$$

$A_f$  is the amplitude of the fast mode, and  $g_q^{(1)}(t)$  is the time correlation function of the scattered electric field at the scattering vector,  $\mathbf{q}(|\mathbf{q}| = (4\pi/\lambda) \sin(\theta/2))$ . Here  $\lambda$  is the wavelength of the light in the medium. The baseline,  $\beta$ , was put equal to  $(1 + A_s)$  for an estimate of  $\Gamma_f$ , where  $A_s$  is the amplitude of the slow mode. On the other hand,  $A_q(t)$  in the long-time domain which corresponded to the slow mode could not be accurately fitted with the cumulant function though the first cumulant itself could be obtained. This is discussed later in detail. Therefore we applied histogram analysis<sup>34</sup> to the data in the long-time domain to obtain the distribution of the decay rate,  $G(\Gamma)$ . The characteristic decay rate,  $\Gamma_s$ , for the slow mode was estimated from  $G(\Gamma)$  with eq 4.

$$\Gamma_s = \int_{\text{slow}} G(\Gamma) \Gamma d\Gamma \quad (4)$$

Eventually  $(1 + A_s)$  was found very close to the stationary value of  $A_q(t)$  appearing over the intermediate time interval. It is to be noted that  $A_s/(A_s + A_f)$  decreases with increasing  $q$ , as is seen in the Figure 3.

**2. The 1.5 wt % PVA Sample.** The PVA concentration of *C* = 1.5 wt % is slightly higher than the overlapping concentration,  $C^* = 1.2$  wt %, which is calculated using previous experimental data (sedimentation and diffusion) of PVA solutions.<sup>35</sup> Figure 2 shows a plot of  $\Gamma_f$  and  $\Gamma_s$  against the square of the scattering vector  $q$  at *T* = 25.0 °C. As mentioned in the previous section, the fast mode was analyzed with the cumulant method and the slow mode by the histogram method. From the figure we see both  $\Gamma_f$  and  $\Gamma_s$  are proportional to  $q^2$ . This indicates that the fast and the slow modes are both the diffusion mode. The diffusion coefficients,  $D_f$  and  $D_s$ , are the respective slopes in the figure. We calculated the hydrodynamic correlation length  $\xi_H$ , which is the dynamical characteristic length of the PVA network from  $D_f$  using eq 5.

$$\xi_H = k_B T / 6\pi\eta_s D_f \quad (5)$$

Here,  $k_B$ , *T*, and  $\eta_s$  are the Boltzmann constant, the

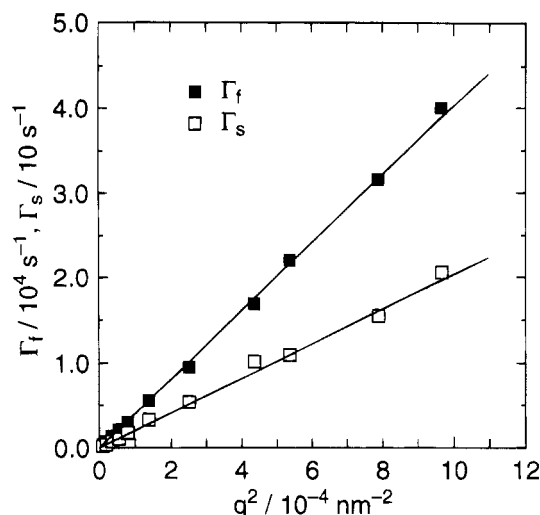


**Figure 2.** Decay rates  $\Gamma_f$  from the fast mode and  $\Gamma_s$  from the slow mode plotted against the square of the scattering vector  $q$  for the sample with  $C = 1.5$  wt % at  $25.0^\circ\text{C}$ . The plot shows that  $\Gamma_f$  and  $\Gamma_s$  are both proportional to  $q^2$ . The slopes of  $\Gamma_f$  and  $\Gamma_s$  give the diffusion coefficients  $D_f$  and  $D_s$ , respectively. Symbols are explained in the figure.

absolute temperature, and the solvent viscosity, respectively. The values are listed in Table 1.  $\xi_H$  takes a value of  $6.5 \text{ nm}$  for  $C = 1.5$  wt %. Values of  $q$  covered with the DLS experiment through  $\theta = 10.4\text{--}150^\circ$  range from  $3.2 \times 10^{-3}$  to  $3.3 \times 10^{-2} \text{ nm}^{-1}$ . Thus  $q\xi_H < 1$  is satisfied for all  $\theta$ , which is consistent with constancy of  $D_f = \Gamma_f/q^2$  over the whole range of  $q$  as is shown in Figure 2. The absolute magnitude of  $D_f = 3.8 \times 10^7 \text{ cm}^2 \text{ s}^{-1}$  suggests that the fast mode corresponds to the cooperative diffusion mode.

On the other hand, the slow mode characterized by the very small diffusion coefficient  $D_s$  might be assigned as the translational diffusion of large particles or clusters composed of many PVA chains physically cross-linked by ol-borate complexes. An estimate of the cluster radius  $r$  from a simple application of eq 5, however, gives a very large value of  $11 \mu\text{m}$ , which is contrary to physical intuition judging from the fact that the solution is clear. At  $C = 1.5$  wt %, slightly higher than the overlapping concentration, the PVA chains slightly overlap one another. Formation of the complexes among overlapped neighboring chains then may produce many clusters of various sizes in the solution and induces a large concentration fluctuation in the spatial scale. Those clusters are further interconnected to one another with a few complexes. If this conjecture were applicable, the association-dissociation kinetics (ADK) of the latter complexes would dominate the diffusion behavior at the long-time end as well as the mechanical behavior in the flow region. The effect of ADK in this semidilute PVA solution results in the diffusion of a large complex in the many surrounding clusters. This is very different from the diffusion of a cluster in dilute solution, where the solvent viscosity is used in eq 5. So we simply replaced the solvent viscosity in eq 5 by the solution viscosity and, on substituting the  $D_s$  value for  $D_f$ , obtained the average cluster size,  $r = 2.4 \times 10^2 \text{ nm}$ , which is about 40 times as large as  $\xi_H$ .

The product  $qr$  is less than unity at low scattering angles and becomes larger than unity at higher scattering angles. Therefore the DLS measurements on this sample prove mainly the translational diffusion of the clusters at low  $\theta$  and prove the local intramolecular

chain motion inside the clusters at high  $\theta$ , which can be characterized by  $D_f$ . Correspondingly, the relative amplitude  $A_s/(A_s + A_f)$  for the slow mode should decrease with increasing  $\theta$ . As is shown in Figure 3,  $A_s/(A_s + A_f)$  rapidly decreases from 0.95 to 0.15 with increasing  $q$  and appears to level off at the large  $q$  end. Our interpretation for the slow mode is not in contradiction with the observed  $q$  dependence of the light intensity. Here we should remark that the size distribution of the clusters in the solution may be broad and also that the number of complexes interconnecting the clusters may vary depending on the cluster size at least. The  $\Gamma$  distribution must be broad. So the histogram method was necessary for data analysis of the slow mode.

Results of dynamic viscoelasticity showed that, in the measured angular frequency range ( $\omega = 0.15\text{--}100 \text{ rad/s}$ ),  $G'(\omega) \sim \omega^2$  and  $G''(\omega) \sim \omega^1$ , which indicates that the sample is in the flow region.<sup>15</sup> We determined the relaxation time,  $\tau_M \sim 0.01 \text{ s}$ , from the slopes of  $G'(\omega)$  and  $G''(\omega)$  using the relations  $G' = G_{NM}\omega^2$  and  $G'' = G_{NM}\omega$ . This relaxation time may be taken as the characteristic time for ADK.

**3. The 1.8 and 2.0 wt % PVA Samples. 3.1. Dynamics at  $25.0^\circ\text{C}$ .** Both the 1.8 and 2.0 wt % PVA samples prepared behaved like very weak gels. Figure 4 shows a plot of  $\Gamma_f$  of 1.8 and 2.0 wt % PVA samples at  $T = 25.0^\circ\text{C}$  against the square of  $q$ . The  $\Gamma_f$  is proportional to  $q^2$  at  $C = 1.8$  and 2.0 wt %. This demonstrates that the fast mode is the diffusion mode as well as at  $C = 1.5$  wt %. The diffusion coefficients,  $D_f$ , are the slope in the figure. We calculated  $\xi_H$  from  $D_f$  using eq 5, and the values are listed in Table 1. The  $\xi_H$  at  $C = 1.8$  wt % was a little smaller than that at  $C = 2.0$  wt %. As in the case of  $C = 1.5$  wt %,  $q\xi_H < 1$  is satisfied for all  $\theta$ , which is consistent with constancy of  $D_f = \Gamma_f/q^2$  over the whole range of  $q$ .  $D_f$  corresponds to the cooperative diffusion coefficient.

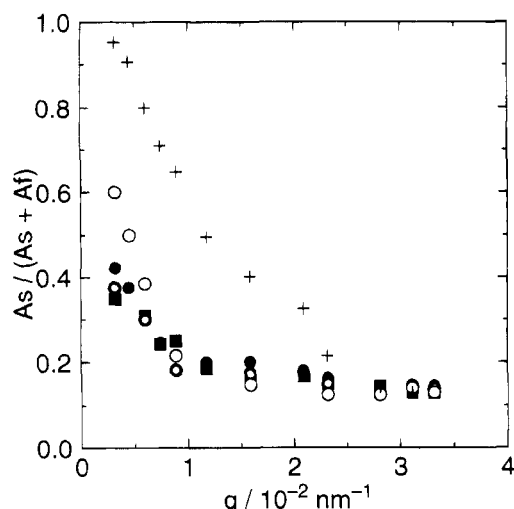
On the other hand, the  $q$  dependence of the slow mode for the two samples was found to be very different from that at the lower concentration of  $C = 1.5$  wt %. The analysis of the  $A_q(t)$  data (in the long-time domain) with the histogram method showed that the  $\Gamma$  distribution was, strictly speaking, better represented by two peaks. The main peak was observed in the same range of the delay times irrespective of  $q$  and the minor peak at the long delay time end. The height of the minor peak was so small in comparison with that of the main peak that, in this paper, we evaluated  $\Gamma_s$  by integration of only the main peak by the use of eq 4. The DLS measurement with a new correlator is in progress, and results of more detailed analysis will be reported soon.

The characteristic decay rate  $\Gamma_s$  of the slow mode is plotted against  $q^2$  at  $T = 25.0^\circ\text{C}$  in Figure 5. The data confirm that  $\Gamma_s$  is independent of  $q$  and indicate that the slow mode is the relaxation mode, not the diffusion mode. The  $\Gamma_s$  appears to decrease with increasing  $C$ , being in contrast with the  $C$  dependence of  $D_f$ . The inverse of  $\Gamma_s$  may be taken as the relaxation time  $\tau_s$ , which characterizes the slow decay of concentration fluctuation. The values are listed in Table 1.

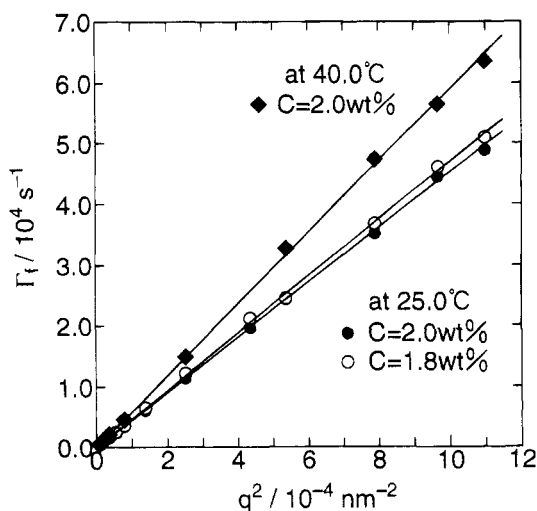
Figure 3 shows the scattering vector dependence of the relative amplitude of the slow mode,  $A_s/(A_s + A_f)$ , for the three samples with  $C = 1.5, 1.8$ , and  $2.0$  wt % at  $25.0^\circ\text{C}$ . The experimental uncertainty for  $A_s$  was about 5%. The relative amplitudes of the  $C = 1.8$  and  $2.0$  wt % samples first decrease with an increase of  $q$  in the range of  $q < 10^{-2} \text{ nm}^{-1}$ , gradually begin to level off with

Table 1. Experimental Results at 25.0 °C

$C/\text{wt } \%$	$D_f/10^{-7} \text{ cm}^2 \text{ s}^{-1}$	$\xi_{H,p}/\text{nm}$	$\Gamma_s/\text{s}^{-1}$	$\tau_s/\text{s}$	$\tau_M/\text{s}$	$G_N/\text{Pa}$	$D_s/10^{-10} \text{ cm}^2 \text{ s}^{-1}$
2.0	$4.50 \pm 0.10$	5.5	$3.6 \pm 0.4$	0.28	$0.24 \pm 0.03$	$210 \pm 10$	
1.8	$4.70 \pm 0.10$	5.2	$12.0 \pm 1.5$	0.08	$0.09 \pm 0.01$	$70 \pm 5$	
1.5	$3.80 \pm 0.10$	6.5			$\sim 0.01$		$2.2 \pm 0.3$



**Figure 3.** Dependence of the relative amplitude of the slow mode  $A_s/(A_s + A_f)$  on the magnitude of the scattering vector  $q$  for the three samples. Symbols for PVA concentration  $C$  at 25.0 °C are (+) 1.5 wt %, (■) 1.8 wt %, and (●) 2.0 wt %, and those for temperature at  $C = 2.0$  wt % are (○) 35.0 °C and (○) 40.0 °C.



**Figure 4.** Decay rates  $\Gamma_f$  from the fast mode plotted against the square of the scattering vector  $q$  for the samples with  $C = 1.8$  wt % at 25.0 °C and  $C = 2.0$  wt % at 25.0 and 40.0 °C. The plot shows that  $\Gamma_f$  are proportional to  $q^2$ .

an increase of  $q$  at intermediate  $q$ , and appears to level off at higher  $q$ .

In order to examine if the slow mode observed in DLS is closely related to the global mechanical relaxation of the PVA/SB network, we made dynamic viscoelastic measurements on the same PVA/SB sample. In Figure 6, we show the angular frequency  $\omega$  dependence of  $G'(\omega)$  and  $G''(\omega)$  of the samples with  $C = 1.8$  and 2.0 wt % at 25.0 °C. The  $G'$  and  $G''$  are proportional to  $\omega^2$  and  $\omega^1$  in the low  $\omega$  region, respectively, which are characteristic of the steady flow behavior.<sup>15</sup> With an increase in  $\omega$ , the frequency dependences of  $G'$  and  $G''$  of the two samples are characterized by a leveling-off of  $G'$  and a maximum of  $G''$ . Such frequency dependences suggest that the relaxation behavior of the PVA/SB complex

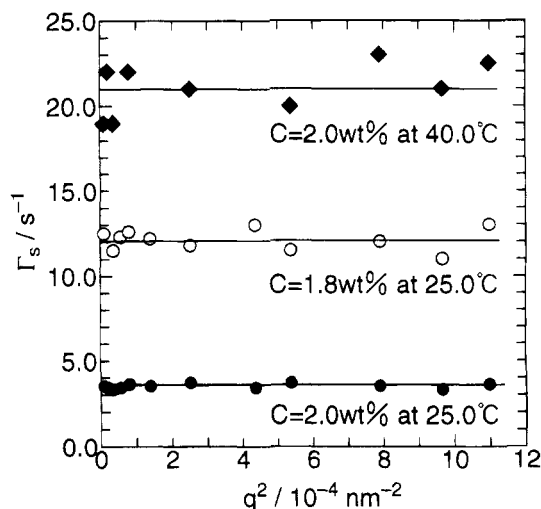


**Figure 5.** Decay rates  $\Gamma_s$  from the slow mode plotted against the square of the scattering vector  $q$  for the samples with  $C = 1.8$  wt % at 25.0 °C and  $C = 2.0$  wt % at 25.0 and 40.0 °C. The plot shows that  $\Gamma_s$  is independent of  $q$ .

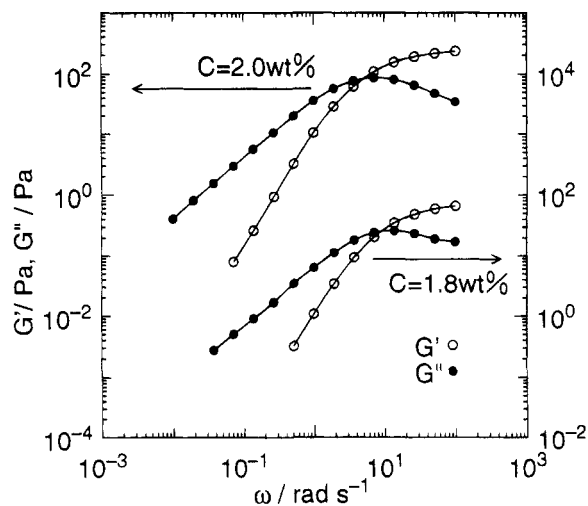


**Figure 6.** Angular frequency  $\omega$  dependence of the storage and the loss shear moduli,  $G'(\omega)$  and  $G''(\omega)$ , of the two samples with  $C = 1.8$  and 2.0 wt % at 25.0 °C. Symbols are explained in the figure. The plateau modulus  $G_N$  and the maximum relaxation time  $\tau_M$  are obtained by fitting eq 6 of the Maxwell model to respective  $G'$  and  $G''$  data.

network on the low- $\omega$  side can be described with a Maxwell model with one relaxation time  $\tau_M$  and the plateau modulus  $G_N$ .

$$G'(\omega) = \frac{G_N \tau_M^2 \omega^2}{1 + \tau_M^2 \omega^2}, \quad G''(\omega) = \frac{G_N \tau_M \omega}{1 + \tau_M^2 \omega^2} \quad (6)$$

We evaluated  $\tau_M$  fitting eq 6 to the respective  $G'$  and  $G''$  data. As is given in Table 1, the characteristic relaxation time  $\tau_s$  from the slow mode is in good agreement with  $\tau_M$ . This result confirms the presence of dynamical coupling between concentration fluctuation and stress in this viscoelastic network system.

The plateau in  $G'$  is observed in the  $\omega$  range of 10–10<sup>2</sup> rad/s. On the other hand, even the smallest decay

Table 2. Experimental Results at  $C = 2.0$  wt %

$T/^\circ\text{C}$	$D_f/10^{-7} \text{ cm}^2 \text{ s}^{-1}$	$\xi_{\text{H}}, \text{nm}$	$\Gamma_f/\text{s}^{-1}$	$\tau_f/\text{s}$	$\tau_M/\text{s}$	$G_N/\text{Pa}$
25.0	$4.50 \pm 0.10$	5.5	$3.6 \pm 0.4$	0.28	$0.24 \pm 0.03$	$210 \pm 10$
35.0	$5.40 \pm 0.10$	5.8	$15.0 \pm 2.0$	0.067	$0.065 \pm 0.005$	$130 \pm 10$
40.0	$5.80 \pm 0.10$	6.0	$21.0 \pm 2.0$	0.048	$0.045 \pm 0.005$	$100 \pm 5$

rate  $\Gamma_f$  for the fast mode to be observed at the lowest scattering angle of  $\theta = 10.4^\circ$  is about  $3 \times 10^2 \text{ s}^{-1}$ , which is larger than the maximum  $\omega = 10^2 \text{ rad/s}$ . Thus, concentration fluctuation in the fast mode decays out, due to the diffusive motion, in a faster time domain. This would confirm that the fast mode was well separated from the slow mode.

**3.2. Temperature Dependence of  $\Gamma_f$  and  $\Gamma_s$  at  $C = 2.0$  wt %.** The DLS and DVE measurements were performed at elevated temperatures of 35.0 and 40.0  $^\circ\text{C}$  on the sample with  $C = 2.0$  wt %. Figures 4 and 5 show plots of  $\Gamma_f$  and  $\Gamma_s$  of the sample at  $T = 40.0$   $^\circ\text{C}$  against  $q^2$ , respectively. The proportionality of  $\Gamma_f$  to  $q^2$  demonstrates that the fast mode at this temperature is the diffusion mode with the diffusion coefficients  $D_f$ . The  $D_f$  increased with increasing temperature. The increase can be mainly attributed to a decrease in the solvent viscosity with increasing temperature. Therefore  $\xi_{\text{H}}$  is a more appropriate quantity for characterization of the physically cross-linked network in the short time scale. At 40.0  $^\circ\text{C}$ ,  $\Gamma_s$  is still independent of  $q$ , indicating that the slow mode is the relaxation mode. From the  $\Gamma_s$  and  $\Gamma_f$  values listed in Table 2,  $\Gamma_s$  is more strongly dependent on  $T$  than  $\Gamma_f$  is.

The  $G'(\omega)$  and  $G''(\omega)$  of the sample with  $C = 2.0$  wt % at 40.0  $^\circ\text{C}$  are found to become proportional to  $\omega^2$  and  $\omega^1$  in the low- $\omega$  region, respectively. The maximum of  $G''$  was also observed as in the case at 25.0  $^\circ\text{C}$ . We evaluated  $\tau_M$  fitting eq 6 to the respective  $G'$  and  $G''$  data. The characteristic relaxation time  $\tau_s$  from the slow mode  $\Gamma_s$  was again in good agreement with  $\tau_M$  at 35.0 and 40.0  $^\circ\text{C}$ . This result confirms that the slow mode proved by DLS is closely related to the viscoelastic nature of the sample.

$G_N$  may be related to the number of complex  $n$ , i.e., the number of physical cross-links, by  $G_N = nk_B T$ .  $n$  may depend on  $T$  like  $n = n_0 \exp(\Delta f/RT)$ , where  $\Delta f$  is the dissociation energy of complex and  $R$  is the gas constant in the measured  $T$  range. The value of  $\Delta f$  can be obtained as the slope from a plot of  $\log(G_N/T)$  vs  $1/T$ . The estimated value of  $\Delta f = 9.0$  kcal/mol is not so different from the activation energy of 6 or 10 kcal/mol for breaking individual cross-links reported by Shultz and Myers<sup>33</sup> as well as the enthalpy of  $-8.5 \pm 1.5$  kcal/mol of formation of a mole of junction points by Shibayama.<sup>36</sup>

**4. Comparison with the Theory.** In previous sections, we saw that the slow decay of concentration fluctuation observed in DLS was the relaxation mode for the samples with  $C = 1.8$  and 2.0 wt % and could be characterized by the relaxation time  $\tau_s$  ( $=\Gamma_s^{-1}$ ). As is clear from Tables 1 and 2, good agreement between  $\tau_s$  and  $\tau_M$  is obtained over the range of  $C$  and  $T$  studied. Therefore we may conclude that the slow mode found in DLS of the PVA/SB complex system is not a local but a global concentration fluctuation. This slow mode is accompanied by the slow relaxation process of the viscoelastic network. It seems important to note that the slow mode exists even in the semidilute solution of good solvent, if the temporary cross-linking points are present.

This slow relaxation mode was first discussed by Brochard and de Gennes. They explained the slow

relaxation mode with a pseudogel model to describe the dynamics of the semidilute solution constituting of high molecular weight polymers.<sup>27,37,38</sup> Their result corresponds to a frozen gel model for which the stress modulus is not allowed to relax. Only in a plateau region where the stress modulus is nearly constant is de Gennes theory expected to be valid. Adam and Delsanti modified the above theory adopting the transient gel model which was able to relax with one relaxation time and also reported an important experimental finding that the fast mode was the collective diffusion mode and the slow one was the relaxation viscoelastic mode which is independent of the scattering vector  $q$ .<sup>24</sup>

Now, there are two theoretical ideas for interpretation of the slow relaxation mode. Theories by a few groups<sup>28,31</sup> predict that mass flow or concentration fluctuation in the gel-like solutions induces deformation of the viscoelastic network, and consequently concentration fluctuation may slowly decay out as the elastic stress generated by the network deformation relaxes. The other theoretical idea is due to Wang.<sup>29,30</sup> As stated in the Introduction, he argues that the difference in partial specific volumes of the polymer and the solvent gives rise to dynamical coupling between concentration fluctuation and density fluctuation and then the viscoelastic mode appears in the DLS power spectrum. These two ideas are essentially incompatible with each other and the physics underlying the slow mode is at issue in the DLS study of viscoelastic polymeric liquids. In this PVA/SB system studied, the partial specific volume of the solvent (water) is 1.00  $\text{cm}^3/\text{g}$  and that of PVA is 0.76  $\text{cm}^3/\text{g}$ , so that the difference in partial specific volumes must be present. Then in our system both the theoretical ideas stated above can explain the slow mode. Here we shall choose the theory of Doi and Onuki<sup>31</sup> for this PVA/SB system for more quantitative discussion, though viscoelasticity was not brought about by chain entanglements but by temporary cross-linking (ADK).

The phenomenological theory developed by Doi and Onuki explains the physics of the dynamical coupling between concentration fluctuation and elastic stress for the entangled polymer solutions as well as polymer blends as follows. Mass flow or concentration fluctuation in the system creates deformation of the viscoelastic network, which produces the gradient of the elastic stress. Then this gradient affects diffusive motion of polymer chains, resulting in slow decay of concentration fluctuation as the network stress relaxes. They predict that the normalized time correlation function  $A_q(t)$  satisfies the following non-Markovian equation:

$$\dot{A}_q(t) + \Gamma_q A_q(t) + (q^2 \xi_{ve}^2 / \eta) \int_0^t dt' G(t-t') \dot{A}_q(t') = 0 \quad (7)$$

Here,  $\dot{A}_q(t) = dA_q(t)/dt$ ,  $\Gamma_q$  is the decay rate for cooperative diffusion without the viscoelastic effect,  $\eta$  is the solution viscosity,  $G(t)$  is the shear modulus at time  $t$ , and  $\xi_{ve}$  is a characteristic length which determines the strength of dynamical coupling. Equation 7 is essentially a phenomenological equation obtained under the important assumptions that (1) the isotropic part

of the network stress is zero and (2) the entanglement network is common to all polymers participating in the entanglement and moves with the tube velocity first proposed by Brochard.<sup>28</sup>

Equation 7 is considerably simplified in the case that the stress relaxation behavior is described by the Maxwell model with the single relaxation time  $\tau_M$  as  $G(t) = G_N \exp(-t/\tau_M)$  in correspondence to the case of our PVA/SB system. Especially, under the conditions of  $\Gamma_q \tau_M \gg 1$  and  $\Gamma_q \tau_M \gg \xi_{ve}^2 q^2$ ,  $A_q(t)$  is calculated to be a sum of two exponential functions,

$$A_q(t) = A_f \exp(-\Gamma_q t) + A_s \exp(-t/\tau_M) \quad (8)$$

$$A_s = (\xi_{ve}^2 q^2 / \Gamma_q \tau_M) / (1 + \xi_{ve}^2 q^2 / \Gamma_q \tau_M), \quad A_f = 1 - A_s \quad (9)$$

The second term on the right-hand side of eq 8 accounts for the viscoelastic effect and is of the order of the shear modulus divided by the bulk modulus, thus being very small in a good solvent. Equation 8 correctly explains not only the time profiles of  $A_q(t)$  shown in Figure 1 but also that the fast mode and the slow mode are the diffusion mode ( $\Gamma_f = \Gamma_q = Dq^2$ ) and the relaxation mode ( $\Gamma_s^{-1} = \tau_s = \tau_M$ ), respectively.

For a more quantitative test of the theory, we calculated  $A_s$  using  $\xi_{ve}^2 = 0.65 \xi_b^2 \eta / \eta_s$  for entangled homopolymer solutions. The  $\xi_b$  is the radius of the so-called blob and may be expressed as  $\xi_b = 1.3 \xi_H$  in the semidilute regime.<sup>17-20</sup> Since  $\Gamma_q (= \Gamma_f)$  has been shown to be accurately proportional to  $q^2$ ,  $\xi_{ve}^2 q^2 / \Gamma_q \tau_M$  becomes independent of  $q$  and is equal to  $5.1 \pi \xi_H^3 \eta / \tau_M k_B T = 0.11$  when  $\xi_H = 5.5$  nm,  $\eta = 40$  Pa s, and  $\tau_M = 0.24$  s are used ( $C = 2.0$  wt %, at 25.0 °C). The theory, thus, gives a  $q$ -independent value of 0.10 as the relative amplitude of the slow mode for the samples. In comparing this prediction with the data shown in Figure 3, we see that agreement between the theory and the experiment is nearly satisfied only for the sample with  $C = 2.0$  wt % at 25.0 °C at high  $q$  and cannot explain the  $q$  and  $T$  dependences of the relative amplitude. From an experimental point of view, we used the linear correlator for the present DLS measurements and superposed two or three raw data with different sampling times to obtain  $A_q(t)$  in Figure 1, which made determination of the relative amplitude ambiguous to some extent. Therefore it seems too early to discuss more about the discrepancy between the theory and the experiment. Now, we are making DLS measurements with a multiple  $\tau$  correlator which covers a broader dynamic range. We shall report on results of numerical analysis of DLS data of this system using a general expression of eq 7 soon.

**Acknowledgment.** We are indebted to Profs. M. Doi and A. Onuki for helpful discussion.

## References and Notes

- (1) Deuel, H.; Neukom, H. *Makromol. Chem.* **1949**, *3*, 13.
- (2) Pezron, E.; Leibler, L.; Richard, L.; Lafuma, F.; Audebert, R. *Macromolecules* **1989**, *28*, 1169.
- (3) Pezron, E.; Richard, L.; Lafuma, F.; Audebert, R. *Macromolecules* **1988**, *21*, 1121.
- (4) Sato, T.; Tsujii, Y.; Fukuda, T.; Miyamoto, T. *Macromolecules* **1992**, *25*, 3890.
- (5) Maerker, J. M.; Sinton, S. W. *J. Rheol.* **1986**, *30*, 77.
- (6) Sinton, S. W. *Macromolecules* **1987**, *20*, 2430.
- (7) Shibayama, M.; Sato, M.; Kurokawa, H.; Fujiwara, H.; Nomura, S. *Polymer* **1988**, *29*, 336.
- (8) Pezron, E.; Richard, L.; Lafuma, F.; Audebert, R. *Macromolecules* **1988**, *21*, 1126.
- (9) Sato, T.; Tsujii, Y.; Fukuda, T.; Miyamoto, T. *Macromolecules* **1992**, *25*, 5970.
- (10) Kurokawa, H.; Shibayama, M.; Ishimaru, T.; Nomura, S.; Wu, W. L. *Polymer* **1992**, *33*, 2182.
- (11) Nickerson, R. F. *J. Polym. Sci.* **1971**, *15*, 111.
- (12) Shibayama, M.; Sato, M.; Kurokawa, H.; Fujiwara, H.; Nomura, S. *Polymer* **1988**, *29*, 336.
- (13) Inoue, T.; Osaki, K. *Rheol. Acta* **1993**, *32*, 550.
- (14) Savin, J. G. *Rheol. Acta* **1968**, *7*, 87.
- (15) Ferry, J. D. *Viscoelastic Properties of Polymers*; John Wiley & Sons Inc.: New York, 1980.
- (16) Nemoto, N.; Kuwahara, M.; Yao, M.; Osaki, K. *Langmuir* **1995**, *11*, 36.
- (17) Doi, M.; Edwards, S. F. *The Theory of Polymer Dynamics*; Oxford University Press: Oxford, 1986.
- (18) Lodge, T. P.; Rotstein, N. A.; Prager, S. *Adv. Chem. Phys.* **1990**, *79*, 1.
- (19) Nemoto, N. In *Polymer Rheology and Processing*; Collyer, A. A., Utracki, L. A., Eds.; Elsevier: London, 1990; p 3.
- (20) Nemoto, N.; Kishine, M.; Inoue, T.; Osaki, K. *Macromolecules* **1990**, *23*, 659; **1991**, *24*, 1648.
- (21) Amis, E. J.; Han, C. C. *Polym. Commun.* **1982**, *23*, 1043.
- (22) Mathies, P.; Mouttet, C.; Weisbuch, G. *J. Phys. (Paris)* **1980**, *41*, 519.
- (23) Nemoto, N.; Makita, Y.; Tsunashima, Y.; Kurata, M. *Macromolecules* **1984**, *17*, 2629.
- (24) Adam, M.; Delasanti, M. *Macromolecules* **1985**, *18*, 1760.
- (25) Brown, W.; Nicolai, T.; Hvidt, S.; Stepanek, P. *Macromolecules* **1990**, *23*, 357.
- (26) Nicolai, T.; Brown, W.; Hvidt, S.; Heller, K. *Macromolecules* **1990**, *23*, 5088.
- (27) Brochard, F.; de Gennes, P.-G. *Macromolecules* **1977**, *10*, 1157.
- (28) Brochard, F. *J. Phys. Fr.* **1983**, *44*, 39.
- (29) Wang, C. H. *J. Chem. Phys.* **1991**, *95*, 3788.
- (30) Wang, C. H. *Macromolecules* **1992**, *25*, 1524.
- (31) Doi, M.; Onuki, A. *J. Phys. II Fr.* **1992**, *2*, 1631.
- (32) Nemoto, N.; Kuwahara, M. *Langmuir* **1993**, *9*, 419.
- (33) Schultz, R. K.; Myers, R. R. *Macromolecules* **1969**, *2*, 281.
- (34) Nemoto, N.; Makita, Y.; Tsunashima, Y.; Kurata, M. *Macromolecules* **1984**, *17*, 425.
- (35) Brandrup, J.; Immergut, E. H. *Polymer Handbook*, 3rd ed.; Wiley-Interscience: New York, 1989.
- (36) Shibayama, M.; Yoshizawa, H.; Kurokawa, H.; Fujiwara, H.; Nomura, S. *Polymer* **1988**, *29*, 2066.
- (37) de Gennes, P.-G. *Macromolecules* **1976**, *9*, 587.
- (38) de Gennes, P.-G. *Scaling Concepts in Polymer Physics*; Cornell University Press: Ithaca, NY, 1979.

MA945071V